



Isotopic Evidence for Glaciation During the Cretaceous Supergreenhouse

André Bornemann, *et al.*

Science **319**, 189 (2008);

DOI: 10.1126/science.1148777

The following resources related to this article are available online at www.sciencemag.org (this information is current as of January 10, 2008):

Updated information and services, including high-resolution figures, can be found in the online version of this article at:

<http://www.sciencemag.org/cgi/content/full/319/5860/189>

Supporting Online Material can be found at:

<http://www.sciencemag.org/cgi/content/full/319/5860/189/DC1>

This article **cites 27 articles**, 10 of which can be accessed for free:

<http://www.sciencemag.org/cgi/content/full/319/5860/189#otherarticles>

This article appears in the following **subject collections**:

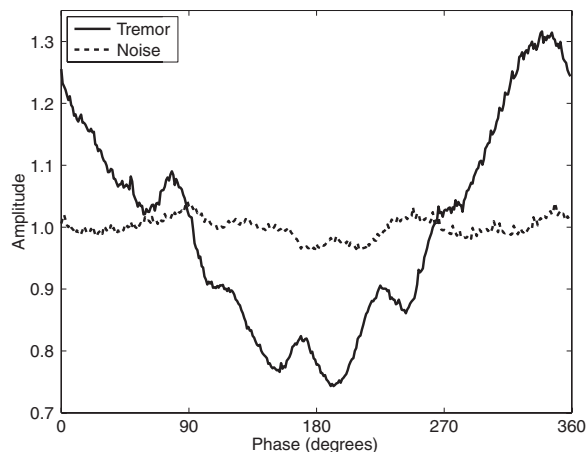
Atmospheric Science

<http://www.sciencemag.org/cgi/collection/atmos>

Information about obtaining **reprints** of this article or about obtaining **permission to reproduce this article** in whole or in part can be found at:

<http://www.sciencemag.org/about/permissions.dtl>

Fig. 4. Amplitude versus phase for a 12.4-hour tidal cycle. In this figure, we compare the variation of the amplitude of tremor during the 13-day ETS windows (solid line) and the 13-day noise windows (dotted line) according to phase in the best-fitting 12.4-hour-period tidal cycle. Phase for each array was determined by cross-correlating a 12.4-hour-period cosine function with the tremor and noise amplitude functions. The amplitude for each degree at each array was averaged over the 25 to 26 times that phase occurred in the 13-day window examined. The amplitudes at the five arrays were averaged for both noise and tremor and were then normalized so that the mean of each curve is 1.



cesses underpinning nonvolcanic tremor are substantially different from those governing earthquakes, which are not typically affected by the tides. ETS appears to represent slow ongoing failure, and thus any increment in stress should affect the failure rate, regardless of the stress state. We believe that this failure is occurring on very weak faults, because small stresses will have a much larger effect on a low-stress fault than a high-stress one. These faults could be very low-friction or, similarly, occur in the presence of near-lithostatic pore pressures.

References and Notes

1. K. Obara, *Science* **296**, 1679 (2002).
2. H. Dragert, K. L. Wang, T. S. James, *Science* **292**, 1525 (2001).
3. M. M. Miller, T. Melbourne, D. J. Johnson, W. Q. Sumner, *Science* **295**, 2423 (2002).

4. G. Rogers, H. Dragert, *Science* **300**, 1942 (2003).
5. K. Obara, H. Hirose, F. Yamamizu, K. Kasahara, *Geophys. Res. Lett.* **31**, L23602 (2004).
6. S. Ide, G. C. Beroza, D. R. Shelly, T. Uchide, *Nature* **447**, 76 (2007).
7. H. Houston, *J. Geophys. Res.* **106**, 11137 (2001).
8. H. Kao *et al.*, *Nature* **436**, 841 (2005).
9. R. M. Nadeau, D. Dolenc, *Science* **307**, 389 (2005).
10. D. R. Shelly, G. C. Beroza, S. Ide, *Nature* **446**, 305 (2007).
11. D. R. Shelly, G. C. Beroza, S. Ide, S. Nakamura, *Nature* **442**, 188 (2006).
12. D. Emter, in *Tidal Phenomena, Lecture Notes in Earth Sciences*, H. Wilhelm, W. Zurn, H.-G. Wenzel, Eds. (Springer-Verlag, Berlin, 1997), vol. 66, pp. 293–309.
13. E. S. Cochran, J. E. Vidale, S. Tanaka, *Science* **306**, 1164 (2004).
14. S. R. McNutt, R. J. Bevan, *Nature* **294**, 615 (1981).
15. W. S. D. Wilcock, *Geophys. Res. Lett.* **28**, 3999 (2001).
16. M. Tolstoy, F. L. Vernon, J. A. Orcutt, F. K. Wyatt, *Geology* **30**, 503 (2002).

17. D. F. Stroup, D. R. Bohnenstiehl, M. Tolstoy, F. Waldhauser, R. T. Weekly, *Geophys. Res. Lett.* **34**, L15301 (2007).
18. M. McNutt, T. H. Heaton, *Calif. Geol.* **34**, 12 (1981).
19. E. S. Cochran, J. E. Vidale, *Geophys. Res. Lett.* **34**, L04302 (2007).
20. J. E. Vidale, D. C. Agnew, M. J. S. Johnston, D. H. Oppenheimer, *J. Geophys. Res.* **103**, 24567 (1998).
21. M. Kennedy, J. E. Vidale, M. Parker, *Seismol. Res. Lett.* **75**, 607 (2004).
22. Materials and methods are available as supporting material on Science Online.
23. D. R. Shelly, G. C. Beroza, S. Ide, *Geochem. Geophys. Geosyst.* **8**, Q10014 (2007).
24. R. Nakata, N. Suda, H. Tsuruoka, *Eos* **87**, Fall Meet. Suppl., Abstract V41A-1700.
25. J. L. Rubinstein *et al.*, *Nature* **448**, 579 (2007).
26. J. Gomberg *et al.*, *Science* **319**, 173 (2008).
27. M. Miyazawa, E. E. Brodsky, paper presented at the Seismological Society of Japan 2007 Fall Meeting, Sendai, Japan, 25 October 2007.
28. M. Miyazawa, J. Mori, *Geophys. Res. Lett.* **32**, L10307 (2005).
29. M. Miyazawa, J. Mori, *Geophys. Res. Lett.* **33**, L05303 (2006).
30. C. W. Ulberg, thesis, Carleton College, Northfield, MN (2007).
31. A summer undergraduate project (30) paved the road for parts of this study. Incorporated Research Institutions for Seismology, Earthscope, and Istituto Nazionale di Geofisica e Vulcanologia provided instruments for the various deployments. D. Agnew provided invaluable help and insight into the tides. J. Sweet assisted with the mapping of the tremor episodes. J. Gomberg, S. Malone, H. Houston, and two anonymous reviewers provided comments that improved this manuscript.

Supporting Online Material

www.sciencemag.org/cgi/content/full/1150558/DC1
Materials and Methods
Figs. S1 and S2

17 September 2007; accepted 13 November 2007
Published online 22 November 2007;
10.1126/science.1150558
Include this information when citing this paper.

Isotopic Evidence for Glaciation During the Cretaceous Supergreenhouse

André Bornemann,^{1,2*} Richard D. Norris,¹ Oliver Friedrich,^{1,3} Britta Beckmann,⁴ Stefan Schouten,⁵ Jaap S. Sinninghe Damsté,⁵ Jennifer Vogel,¹ Peter Hofmann,⁴ Thomas Wagner⁶

The Turonian (93.5 to 89.3 million years ago) was one of the warmest periods of the Phanerozoic eon, with tropical sea surface temperatures over 35°C. High-amplitude sea-level changes and positive $\delta^{18}\text{O}$ excursions in marine limestones suggest that glaciation events may have punctuated this episode of extreme warmth. New $\delta^{18}\text{O}$ data from the tropical Atlantic show synchronous shifts ~91.2 million years ago for both the surface and deep ocean that are consistent with an approximately 200,000-year period of glaciation, with ice sheets of about half the size of the modern Antarctic ice cap. Even the prevailing supergreenhouse climate was not a barrier to the formation of large ice sheets, calling into question the common assumption that the poles were always ice-free during past periods of intense global warming.

Despite the extreme warmth of the Turonian (1–3) [93.5 to 89.3 million years ago (Ma) (4)], it has been argued that there may have been several stages of continental ice growth during the period, reflected in both erosional surfaces and geochemical records associated with possible glaciation-induced sea-level

falls (5–7). Rapid decreases (<1 million years) in sea level are known from diverse locations in the Turonian of northern Europe, North America, and the Russian Platform and are estimated at magnitudes of 25 to 40 m (7, 8) or even more (9). These rapid changes in sea level are too fast and too widespread to be accounted for by tec-

tonic processes and were therefore plausibly triggered by glacioeustasy (7, 10). Further evidence comes from positive $\delta^{18}\text{O}$ excursions in marine, but diagenetically altered, limestone sequences (5, 11) and brachiopod isotope data (6). However, evidence from sedimentological findings such as ice-rafted debris is still lacking, and unequivocal $\delta^{18}\text{O}$ records of well-preserved open-ocean foraminifera are rare, are of low resolution, or do not support the idea of Late Cretaceous ice sheets (12). Moreover, there is only a poor understanding of how large ice sheets might grow in a period when tropical sea surface temperatures (SSTs) exceed 35°C (3, 13) and high-latitude temperatures are in excess of 20°C (2, 14).

We used two independent techniques to estimate SSTs during the early Late Cretaceous. One proxy is the $\delta^{18}\text{O}$ paleothermometer, which we applied to monospecific planktic foraminiferal samples from a 40-m-thick, organic carbon-rich, laminated marlstone succession of Turonian to Santonian age from the western equatorial Atlantic at Demerara Rise [Ocean Drilling Program (ODP) Site 1259]. These sediments contain planktic foraminifera with a “glassy” appearance and pristine, well-preserved wall textures (15).

This state of preservation is ideal for an extensive geochemical investigation in order to reconstruct past SSTs (16). Comparison of the $\delta^{18}\text{O}$ values of planktic and benthic foraminifera was also used to provide information on the global isotopic composition of oceans when compared against a salinity-independent temperature proxy: the tetraether index of lipids with 86 carbon atoms (TEX_{86}), which is based on the distribution of crenarchaeol membrane lipids (17, 18). Because the growth of continental ice enriches seawater in ^{18}O , the $\delta^{18}\text{O}$ chemistry, when constrained by TEX_{86} temperature estimates, can be further used to estimate the size of continental ice sheets.

Our tropical $\delta^{18}\text{O}$ -derived SST estimates range from $\sim 34^\circ$ to $\sim 37^\circ\text{C}$ [-4.2 to -4.9 per mil (‰), Vienna Pee Dee belemnite (VPDB) standard] in the Turonian and from $\sim 31.5^\circ$ to $\sim 35^\circ\text{C}$ (-3.65 to -4.4% VPDB) in the late Coniacian and Santonian (Fig. 1A). These values are in good agreement with earlier estimates from spot measurements from the western Atlantic (1, 3) and with low-resolution data from the organic paleothermometer TEX_{86} (13). Newly generated TEX_{86} data indicate high SSTs of up to 36°C during the Turonian, followed by a shift to cooler temperatures during the Coniacian and Santonian (Fig. 1B). Today, temperatures in the western tropical Atlantic range from 28° to 29°C (19), so our data suggest that the Turonian surface ocean was 5° to 9°C warmer than at present.

The Turonian warmth was punctuated by a short-lived decrease in the $\delta^{18}\text{O}$ content of planktic foraminifera ~ 91.34 Ma [523 meters of composite depth (mcd)] and a pronounced positive $\delta^{18}\text{O}$ excursion centered on the CC11/CC12 calcareous nannofossil biozone boundary ~ 91.2 Ma (521.5 mcd) (Figs. 1A and 2A). The most negative $\delta^{18}\text{O}$ ratios in our record are found ~ 91.34 Ma, but the implied SST peak ($>36^\circ\text{C}$) is not reflected in either the benthic foraminiferal $\delta^{18}\text{O}$ or the TEX_{86} data (Fig. 2). Evidently, this $\delta^{18}\text{O}$ event reflects an episode of acceleration of the hydrological cycle, causing a decrease in the local sea surface salinity (Fig. 2C), and was followed at ~ 91.2 Ma by a synchronous positive shift in $\delta^{18}\text{O}$ in both planktic and benthic foraminifera, which lasted for $\sim 200,000$ years. The magnitude of the positive $\delta^{18}\text{O}$ excursion in planktic foraminifera is $>1\%$, whereas it is up to 0.7% in benthic foraminifera.

Because TEX_{86} temperature estimates are independent of changes in seawater $\delta^{18}\text{O}$ (δ_w), we calculated temperature anomalies based on paired measurements of both $\delta^{18}\text{O}$ and TEX_{86} to quantify the change in δ_w (Fig. 2C) produced by the possible growth of continental ice. The TEX_{86} data display only a 1°C decrease in surface ocean temperatures associated with the 91.2 Ma planktic oxygen isotope shift. Therefore the remaining 0.4 to 0.6% anomaly during the 91.2 Ma event in planktic foraminiferal $\delta^{18}\text{O}$, which is similar to the range suggested by the benthic foraminifera (0.3 to 0.7%), must primarily reflect changes in δ_w rather than ocean temperature alone. Both the surface ocean and the deep sea floor (estimated to be at depths >1500 m) (20) show the positive $\delta^{18}\text{O}$ anomaly, making it unlikely that this signal reflects local changes in surface ocean salinity. It is much more likely that the synchronous change in benthic and planktic foraminiferal $\delta^{18}\text{O}$ was produced by sequestering ^{16}O in glacial ice, causing a whole-ocean increase in δ_w .

The middle Turonian is characterized by a series of short-term relative sea-level changes

(9, 21) that are consistent with our glacioeustatic interpretation of the isotopic record. Two major widespread unconformities, Tu-2 at 91.2 Ma and Tu-3 at 90.9 Ma (21, 22), correspond to sea-level falls of at least 25 m (9, 21) and occur close to the CC11/CC12 nannofossil zone boundary (91.2 Ma) (4). Data from the Russian Platform (8) suggest a drop in sea level of up to 40 m at ~ 91 Ma, and a further drop by ~ 25 to 30 m is reported from the New Jersey margin at the CC11/CC12 boundary (7, 10). The sea-level record from the Russian Platform is particularly important because this region is generally regarded as tectonically stable, making it a particularly good place to estimate global sea-level changes. A large-scale unconformity has also been reported from the Western Interior Basin (23) and northwest Europe (24) in the late middle Turonian. Because of stratigraphic uncertainties and the lack of sophisticated supraregional stratigraphic concepts, it is not clear which of these unconformities correspond to the observed positive $\delta^{18}\text{O}$ shift. However, the widespread occurrence of high-amplitude relative sea-level changes sup-

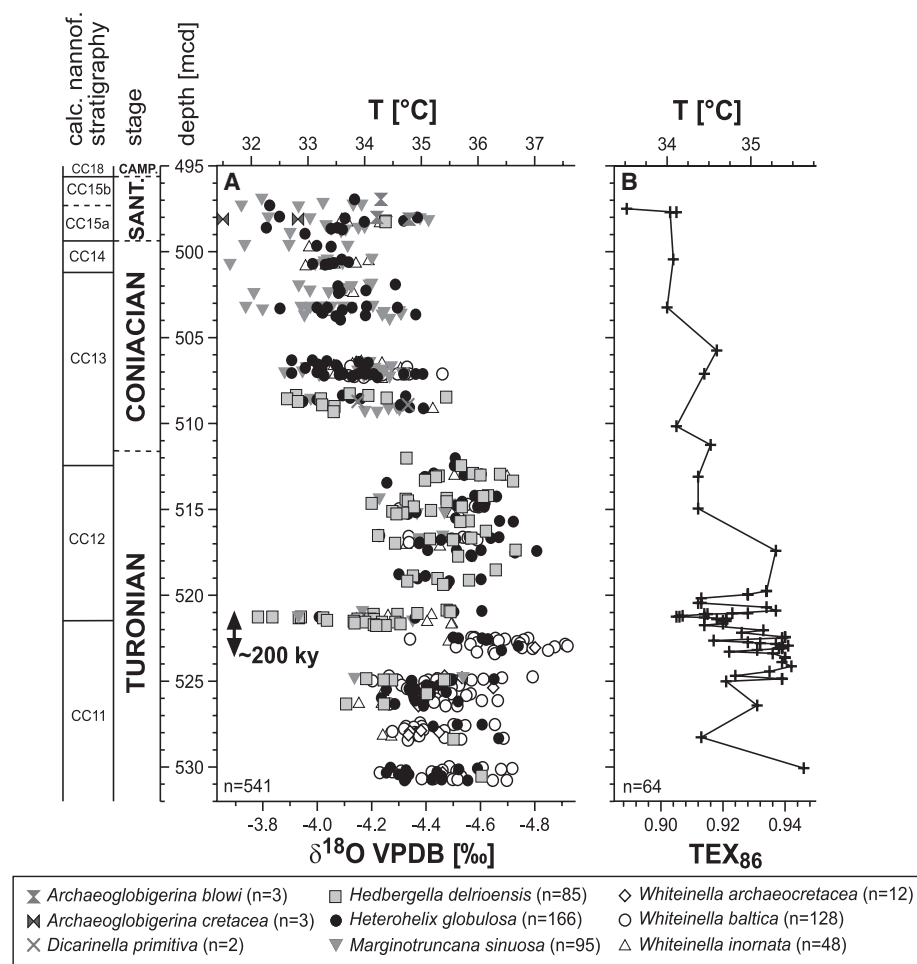


Fig. 1. Stratigraphy and calculated SSTs based on planktic foraminiferal $\delta^{18}\text{O}$ and TEX_{86} data for the Turonian to Santonian interval at ODP Site 1259 (33), Demerara Rise, western equatorial Atlantic. (A) $\delta^{18}\text{O}$ data based on monospecific planktic foraminiferal and corresponding conservative SST estimates. (B) TEX_{86} values and the calculated SSTs. The late Turonian $\delta^{18}\text{O}$ peak interval is estimated to represent $\sim 200,000$ years (200 ky). T, temperature.

¹Scripps Institution of Oceanography, University of California, San Diego, Geosciences Research Division, 9500 Gilman Drive, La Jolla, CA 92093-0244, USA. ²Institut für Geophysik und Geologie, Universität Leipzig, Talstraße 35, D-04103 Leipzig, Germany. ³School of Ocean and Earth Science, National Oceanography Centre, European Way, Southampton SO14 3ZH, UK. ⁴Institut für Geologie und Mineralogie, Universität Köln, Zùlpicher Straße 49a, D-50674 Köln, Germany. ⁵Department of Marine Biogeochemistry and Toxicology, Royal Netherlands Institute for Sea Research, Post Office Box 59, 1790 AB Den Burg, Texel, Netherlands. ⁶School of Civil Engineering and Geosciences, Newcastle University, Newcastle upon Tyne NE1 7RU, UK.

*To whom correspondence should be addressed. E-mail: a.bornemann@uni-leipzig.de

ports the hypothesis that continental ice may have formed in the middle Turonian. Our biostratigraphy and the $\delta^{13}\text{C}$ record (fig. S2) suggest that the positive $\delta^{18}\text{O}$ shift is synchronous with the Pewsey Event in western Europe (25, 26), which is considered to have been associated with regional cooling based on bulk-rock $\delta^{18}\text{O}$ data and faunal patterns from western Europe (11).

The magnitude of the sea-level fall associated with the 91.2 Ma $\delta^{18}\text{O}$ shift is constrained by four variables: (i) our 0.3 to 0.7‰ δ_{W} anomaly, (ii) the magnitude of the late Turonian sea-level fall [–25 to 40 m (7, 8)], (iii) an estimate of the relationship between sea level and $\delta^{18}\text{O}$ [0.11‰ VPDB $\delta^{18}\text{O}$ per 10 m of sea-level fall in the Quaternary (27) and 0.075‰ VPDB $\delta^{18}\text{O}$ per 10 m of sea-level fall in a warm climate scenario (7)], and (iv) the estimated $\delta^{18}\text{O}$ composition of Cretaceous ice. The first three variables are well known, whereas the isotopic composition of Cretaceous ice can be constrained between the average modern value for the Antarctic ice cap [–44‰ Vienna standard mean ocean water (VSMOW)] (7) and the predicted ice composition for past warm climates (–30‰

VSMOW) (7, 28). Given the modern $\delta^{18}\text{O}$ composition of the Antarctic ice cap, the observed $\delta^{18}\text{O}$ anomaly is consistent with a sea-level fall of 27 to 64 m. Today, the Antarctic ice sheet stores sufficient water to change global sea level by 61 m (29). Therefore, our calculated volume of the Cretaceous ice sheet is equivalent to 44 to 105% that of the modern Antarctic ice sheet. If Cretaceous ice had a $\delta^{18}\text{O}$ composition of –30‰ VSMOW, the 91.2 Ma event would be consistent with a sea-level fall of 40 to 93 m and an ice volume 66 to 152% that of modern Antarctica.

We propose that any large Turonian ice sheet was probably located on Antarctica, given the polar position of the continent and the widespread areas of elevated terrain (with altitudes of 1500 to 2500 m) when the modern ice cap is isostatically removed (30). However, the uplift history of the Transantarctic Mountains before the Cenozoic is very poorly known and may have commenced during the Cretaceous (31) or the Eocene (32). Warm tropical and subpolar SSTs in the Turonian (1–3) would seem to preclude substantial ice development at or near sea level, even on Antarctica, emphasizing the need for

further work on the paleoelevation history of the continent.

It is unlikely that an ice sheet of the size of the modern Antarctic ice cap existed in the Cretaceous, both because of the warm surface temperatures noted above and because there is no evidence for the ice-raftered debris that should be present in the Southern Ocean if all of Antarctica had been glaciated. However, an ice cap of up to ~60% the size of the modern Antarctic ice sheet is plausible given the constraints imposed by the sea-level record, as well as our estimate of the change in mean ocean δ_{W} , and our –44‰ VSMOW estimate for the isotopic composition of glacial ice. These results also imply that the $\delta^{18}\text{O}$ composition of Turonian polar precipitation was not substantially heavier than today and contradict expectations that greenhouse warming should decrease fractionation during vapor transport from mid- to high latitudes (7, 28).

We are left with the apparent paradox that the prevailing extraordinarily high tropical temperatures during the Turonian were not a barrier to the initiation and growth of large continental ice sheets. The development of these ice sheets could be attributed to an increase in the activity of the hydrological cycle, which must have initiated more humid conditions and enhanced precipitation in the high latitudes. As with periods of Cenozoic ice growth, the initiation of Cretaceous ice expansion may have been triggered by orbital dynamics, because the ~200,000-year duration of the 91.2 Ma event is similar to the half period of the 400,000-year eccentricity cycle. Our results suggest that fairly large ice sheets could grow and decay equally rapidly, which is very much the same pattern as during the Pleistocene. However, unlike the Pleistocene, Cretaceous ice sheets were apparently not a regularly recurring phenomenon, possibly because the extreme warmth of the Turonian, the paleoelevation of Antarctica, and the orbital configuration allowed the initiation of ice sheet development only under certain rare conditions. Our results further suggest that the common assumption that ice sheets did not exist during periods of past supergreenhouse climates should be reexamined, with implications for paleotemperature estimation, the determination of the past isotopic composition of seawater, and high-latitude terrestrial climate reconstruction.

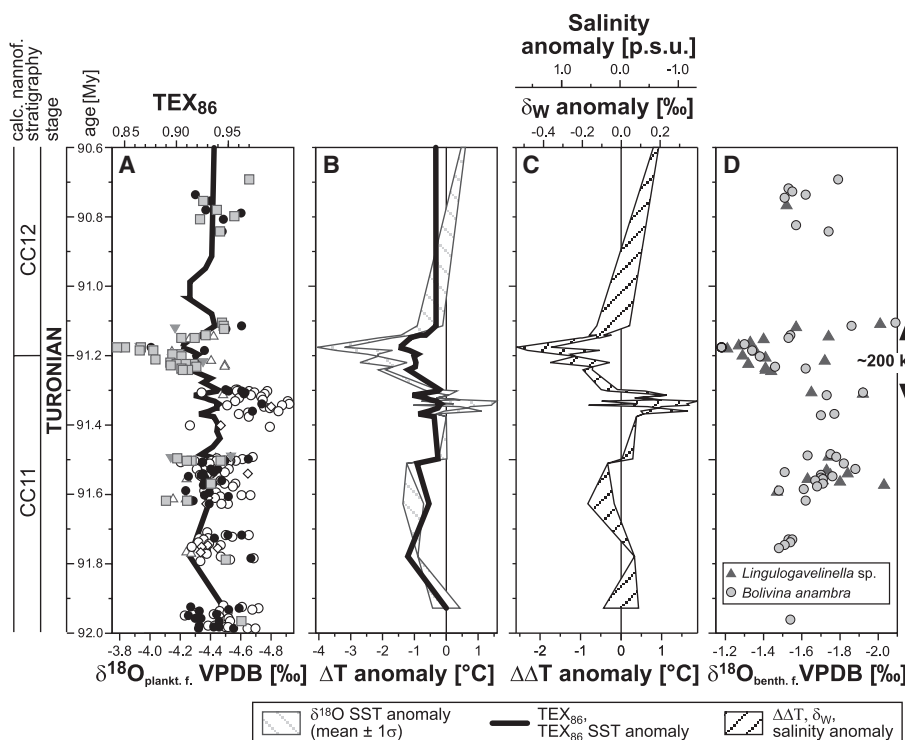


Fig. 2. Detailed data from the CC11 and CC12 calcareous nannofossil biozone interval of ODP Site 1259 (33). Data are plotted against absolute age (4) (table S1) and cover the interval from 518.02 to 530.78 mcd in Fig. 1. (A) The raw planktic foraminiferal $\delta^{18}\text{O}$ data (see Fig. 1 for symbol explanation) and TEX_{86} data; both are plotted on the same scale with respect to the estimated SSTs in Fig. 1. (B) $\delta^{18}\text{O}$ and TEX_{86} anomalies were calculated in reference to sample 1259B-22-4, 75–76.5 cm (530.08 mcd, 91.93 My). In (B) and (C), only those samples are shown from which both proxy data types ($\delta^{18}\text{O}$ and TEX_{86}) are available. These anomalies were then converted to expected δ_{W} anomalies (C) by application of a $\delta^{18}\text{O}/T$ relationship of $-0.208\text{‰}/^{\circ}\text{C}$. The resulting δ_{W} anomaly was then assumed to reflect changes corresponding to surface water salinity changes due to shifts in the precipitation/evaporation balance. The salinity anomaly field represents a δ_{W} /salinity relationship of 0.30‰/practical salinity units (p.s.u.) (33). (D) $\delta^{18}\text{O}$ data from two benthic foraminiferal taxa show a positive $\delta^{18}\text{O}$ shift of 0.3 to 0.7‰ within ~200,000 years, which parallels the δ_{W} anomaly.

References and Notes

- P. A. Wilson, R. D. Norris, M. J. Cooper, *Geology* **30**, 607 (2002).
- K. L. Bice, B. T. Huber, R. D. Norris, *Paleoceanography* **18**, 10.1029/2002PA000848 (2003).
- K. L. Bice *et al.*, *Paleoceanography* **21**, 10.1029/2005PA001203 (2006).
- F. Gradstein, J. Ogg, A. Smith, Eds., *A Geologic Time Scale 2004* (Cambridge Univ. Press, Cambridge, 2004).
- H. M. Stoll, D. P. Schrag, *Geol. Soc. Am. Bull.* **112**, 308 (2000).
- S. Voigt, A. S. Gale, S. Flögel, *Paleoceanography* **19**, 10.1029/2004PA001015 (2004).
- K. G. Miller, J. D. Wright, J. V. Browning, *Mar. Geol.* **217**, 215 (2005).

8. D. Sahagian, O. Pinous, A. Olferiev, V. Zakharov, *Am. Assoc. Pet. Geol. Bull.* **80**, 1433 (1996).
9. B. U. Haq, J. Hardenbol, P. R. Vail, *Science* **235**, 1156 (1987).
10. K. G. Miller *et al.*, *Science* **310**, 1293 (2005).
11. S. Voigt, F. Wiese, *J. Geol. Soc.* **157**, 737 (2000).
12. B. T. Huber, R. D. Norris, K. G. MacLeod, *Geology* **30**, 123 (2002).
13. A. Forster, S. Schouten, M. Baas, J. S. Sinninghe Damsté, *Geology* **35**, 919 (2007).
14. A. B. Herman, R. A. Spicer, *Nature* **380**, 330 (1996).
15. A. Bornemann, R. D. Norris, *Mar. Micropaleontol.* **65**, 32 (2007).
16. P. N. Pearson *et al.*, *Nature* **413**, 481 (2001).
17. S. Schouten, E. C. Hopmans, E. Schefuss, J. S. Sinninghe Damsté, *Earth Planet. Sci. Lett.* **204**, 265 (2002).
18. C. Wuchter, S. Schouten, M. J. L. Coolen, J. S. Sinninghe Damsté, *Paleoceanography* **19**, 10.1029/2004PA001041 (2004).
19. J. I. Antonov, S. Levitus, T. P. Boyer, M. E. Conkright, T. O'Brien, *World Ocean Atlas 1998* (National Oceanic and Atmospheric Administration, Silver Spring, MD, 1998), vol. 1.
20. M. A. Arthur, J. H. Natland, in *Deep Drilling Results in the Atlantic Ocean: Continental Margins and Paleoenvironment*, M. Talwani, W. W. Hay, W. B. F. Ryan, Eds. (American Geophysical Union, Washington, DC, 1979), pp. 375–401.
21. J. Hardenbol, J. Thierry, M. B. Farley, P.-C. De Graciansky, P. R. Vail, in *Mesozoic and Cenozoic Sequence Chronostratigraphic Framework of European Basins*, P. C. De Graciansky, J. Hardenbol, T. Jacquin, P. Vail, Eds. (Society for Sedimentary Geology, Tulsa, OK, 1998), vol. 60, pp. 3–13.
22. Absolute ages are adopted from TSCreator (www.stratigraphy.org), based on (21), recalibrated after (4).
23. B. B. Sageman, J. Rich, M. A. Arthur, G. E. Birchfield, W. E. Dean, *J. Sediment. Res.* **67**, 286 (1997).
24. J. M. Hancock, *Proc. Geol. Assoc.* **100**, 565 (1989).
25. A. S. Gale, *Geol. Soc. Spec. Publ.* **103**, 177 (1996).
26. I. Jarvis, A. S. Gale, H. C. Jenkyns, M. A. Pearce, *Geol. Mag.* **143**, 561 (2006).
27. R. G. Fairbanks, R. K. Matthews, *Quat. Res.* **10**, 181 (1978).
28. H. K. Coxall, P. A. Wilson, H. Pälike, C. H. Lear, J. Backman, *Nature* **433**, 53 (2005).
29. P. Huybrechts, D. Steinhage, F. Wilhelms, J. Bamber, *Ann. Glaciol.* **30**, 52 (2000).
30. R. M. DeConto, D. Pollard, *Nature* **421**, 245 (2003).
31. P. Fitzgerald, *Roy. Soc. New Zeal. Bull.* **35**, 453 (2002).
32. U. S. ten Brink, R. I. Hackney, S. Bannister, T. A. Stern, Y. Makovsky, *J. Geophys. Res.* **102**, 27603 (1997).
33. Materials, methods, and data are available as supporting material on Science Online.
34. This research used samples and data provided by the ODP. The ODP was sponsored by NSF and participating countries under the management of Joint Oceanographic Institutions (JOI). We thank P. Worstell for sample preparation and C. Charles (Scripps Institution of Oceanography) and D. Andreasen (University of California Santa Cruz) for their assistance with the mass spectrometers. Financial support was provided by the German Research Foundation (A.B., O.F., and T.W.) and JOI/U.S. Science Support Program (R.D.N.). T.W. acknowledges the Royal Society–Wolfson Research Merit Award.

Supporting Online Material

www.sciencemag.org/cgi/content/full/319/5860/189/DC1

Materials and Methods

Figs. S1 and S2

Tables S1 to S4

References and Notes

3 August 2007; accepted 16 November 2007

10.1126/science.1148777

Breakdown of an Ant-Plant Mutualism Follows the Loss of Large Herbivores from an African Savanna

Todd M. Palmer,^{1,2,4*} Maureen L. Stanton,^{2,3,4} Truman P. Young,^{2,4,5} Jacob R. Goheen,^{1,4,6} Robert M. Pringle,^{4,7} Richard Karban⁸

Mutualisms are key components of biodiversity and ecosystem function, yet the forces maintaining them are poorly understood. We investigated the effects of removing large mammals on an ant-*Acacia* mutualism in an African savanna. Ten years of large-herbivore exclusion reduced the nectar and housing provided by plants to ants, increasing antagonistic behavior by a mutualistic ant associate and shifting competitive dominance within the plant-ant community from this nectar-dependent mutualist to an antagonistic species that does not depend on plant rewards. Trees occupied by this antagonist suffered increased attack by stem-boring beetles, grew more slowly, and experienced doubled mortality relative to trees occupied by the mutualistic ant. These results show that large mammals maintain cooperation within a widespread symbiosis and suggest complex cascading effects of megafaunal extinction.

Obligate mutualistic relationships among species are ubiquitous and central to ecological function and the maintenance of biodiversity (1–5). The symbiosis between ants and plants, which involves many species throughout the tropics, was the first coevolved mutualism to be thoroughly elucidated by ecol-

ogists (6). Many studies have shown the efficacy of ant mutualists in deterring herbivory (7) and explored the costs and benefits accruing to the interacting partners (8). However, although the importance of large herbivores in the evolution and maintenance of these interactions has been hypothesized (9, 10), it has never been shown.

We investigated the effects of large mammalian herbivores on an ant-*Acacia* mutualism in an African savanna. The whistling-thorn tree, *Acacia drepanolobium*, dominates heavy-clay soils across large expanses of upland East Africa (11). At branch nodes, *A. drepanolobium* produces either slender stipular thorns or hollow swollen thorns that serve as ant housing (“domatia”). The tree also secretes a carbohydrate-rich nectar from extrafloral glands located near the bases of leaves (12). At our study site in Kenya, four species of ants (*Crematogaster mimosae*,

C. sjostedti, *C. nigriceps*, and *Tetraponera penzigi*) compete for exclusive possession of host trees and vary strongly in both their defense of the host trees and their use of the tree’s “rewards” [i.e., domatia and nectar (11, 13)]. *Crematogaster mimosae* aggressively defends host trees from herbivores and relies heavily on swollen-thorn domatia, where they raise brood, house workers, and occasionally tend honeydew-producing scale insects (Coccidae) (11). In contrast, *C. sjostedti* is a less-aggressive defender of host plants (13) and, exclusively among the four ant species, does not nest in domatia but rather in stem cavities excavated by the larvae of long-horned beetles (Cerambycidae). Under natural conditions, *C. mimosae* is the most abundant ant symbiont, occupying ~52% of all trees at our sites, whereas *C. sjostedti* occupies ~16% of host plants.

The remaining two ant species, *C. nigriceps* and *T. penzigi*, also occur in relatively low abundance (~15% and ~17% of trees, respectively), and each uses distinctive behaviors that reduce the likelihood of hostile takeover by the competitively superior *C. mimosae* and *C. sjostedti*. *Crematogaster nigriceps* is an effective defender (13, 14) but also prunes axillary buds and kills apical meristems, which reduces lateral canopy spread and thus the likelihood of contact with trees occupied by hostile colonies (15). *Tetraponera penzigi*, an intermediate protector, destroys its host-plants’ nectaries: a “scorched-earth” strategy that reduces the probability of takeover by neighboring nectar-dependent *Crematogaster* colonies (16). All three *Crematogaster* species derive at least some of their energy by foraging off-tree for insects; in contrast, *T. penzigi* seldom leaves its host and appears to subsist by gleaning small food items (e.g., pollen and fungal spores) from the surfaces of its host (17).

In 2005, we sampled *A. drepanolobium* trees (1.8 to 3.0 m in height) in 12 plots (4 ha each)

¹Department of Zoology, University of Florida, Gainesville, FL 32611, USA. ²Center for Population Biology, University of California, Davis, CA 95616, USA. ³Section of Evolution and Ecology, University of California, Davis, CA 95616, USA. ⁴Mpala Research Centre, Box 555, Nanyuki, Kenya. ⁵Department of Plant Environmental Sciences, University of California, Davis, CA 95616, USA. ⁶Department of Zoology, University of British Columbia, Vancouver, BC V6T 1Z4, Canada. ⁷Department of Biological Sciences, Stanford University, Stanford, CA 94305, USA. ⁸Department of Entomology, University of California, Davis, CA 95616, USA.

*To whom correspondence should be addressed. E-mail: tmpalmer@zoo.ufl.edu